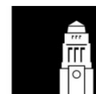

UNIVERSITY OF LEEDS

This is a repository copy of *Non-Invasive Millimeter-Wave Profiler for Surface Height Measurement of Photoresist Films*.

White Rose Research Online URL for this paper:
http://eprints.whiterose.ac.uk/126916/

Version: Accepted Version

Article:

Chudpooti, N, Doychinov, V orcid.org/0000-0001-6730-0057, Akkaraekthalin, P et al. (2 more authors) (2018) Non-Invasive Millimeter-Wave Profiler for Surface Height Measurement of Photoresist Films. IEEE Sensors Journal, 18 (8). pp. 3174-3182. ISSN 1530-437X

https://doi.org/10.1109/JSEN.2018.2806185

© 2018 IEEE. This is an author produced version of a paper published in IEEE Sensors Journal. Personal use of this material is permitted. Permission from IEEE must be obtained for all other uses, in any current or future media, including reprinting/republishing this material for advertising or promotional purposes, creating new collective works, for resale or redistribution to servers or lists, or reuse of any copyrighted component of this work in other works. Uploaded in accordance with the publisher's self-archiving policy.

Reuse
Items deposited in White Rose Research Online are protected by copyright, with all rights reserved unless indicated otherwise. They may be downloaded and/or printed for private study, or other acts as permitted by national copyright laws. The publisher or other rights holders may allow further reproduction and re-use of the full text version. This is indicated by the licence information on the White Rose Research Online record for the item.

Takedown
If you consider content in White Rose Research Online to be in breach of UK law, please notify us by emailing eprints@whiterose.ac.uk including the URL of the record and the reason for the withdrawal request.

eprints@whiterose.ac.uk
https://eprints.whiterose.ac.uk/

Non-Invasive Millimeter-Wave Profiler for Surface Height Measurement of Photoresist Films

Journal:	*IEEE Sensors Journal*
Manuscript ID	Sensors-20623-2018
Manuscript Type:	Regular Paper
Date Submitted by the Author:	12-Jan-2018
Complete List of Authors:	Chudpooti, Nonchanutt; King Mongkut's University of Technology North Bangkok, Department of Electrical and Computer Engineering Doychinov, Viktor; University of Leeds, Institute of Robotics, Autonomous Systems, and Sensing Akkaraekthalin, Prayoot; King Mongkut\'s University of Technology North Bangkok, Faculty of Engineering Robertson, Ian; Leeds University, Electrical and Electronic Dept. Somjit, Nutapong; University of Leeds, School of Electronic and Electrical Engineering
Keywords:	MICR

SCHOLARONE™
Manuscripts

For Review Only

Non-Invasive Millimeter-Wave Profiler for Surface Height Measurement of Photoresist Films

Nonchanutt Chudpooti, Student Member, IEEE, Viktor Doychinov, Member, IEEE,
Prayoot Akkaraekthalin, Member, IEEE, Ian D. Robertson, Fellow, IEEE, and Nutapong Somjit, Member, IEEE

Abstract — This work presents a low-cost non-invasive millimeter-wave surface-height measurement sensor of dielectric and polymer films on glass and quartz substrates. The surface-height profiler utilizes near-field resonance measurement technique operating at 96 GHz implemented by using a single complementary split-ring resonator (CSRR) integrated with a tailor-made WR10 rectangular waveguide. By placing a glass or quartz substrate uniformly coated with SU-8 photoresist on top of the CSRR, the thickness of the SU-8 polymer can be extracted based on the reflected and transmitted electromagnetic-wave energy interacting at the electrical boundary between the substrate and polymer film. Uniform single layers of SU-8 polymer with thicknesses from 3 to 13 µm, coated on top of glass substrate are measured and characterized. The extracted polymer-film thicknesses from the sensor in this work show an agreement of higher than 95% as compared to the commercial surface profiler instrument, while offering various advantages e.g. non-invasion, ease of measurement setup, low-cost and miniaturization.

Index Terms—non-invasive measurement, millimeter-wave sensor, thickness characterization, SU-8 photoresist, W-band.

I. Introduction

NON-DESTRUCTIVE measurement of dielectric and polymer structures with varying layer thicknesses and relative permittivity offer valuable information when characterizing these structures in a multitude of fabrication processes and quality control applications, such as on-wafer thin-film coating thickness, microfabrication of micro-electromechanical systems (MEMS), biomedical applications such as joint replacements protective coatings, and material science for purposes of material characterization [1]-[6], [19].

This work was supported in part by the Engineering and Physical Sciences Research Council (EPSRC) under Grant EP/N010523/1, in part by the Thailand Research Fund through the TRF Senior Research Scholar Program under Grant RTA6080008, in part by the Royal Golden Jubilee Ph.D. Program under Grant PHD/0093/2557.

N. Chudpooti and P. Akkaraekthalin are with the Department of Electrical and Computer Engineering, Faculty of Engineering, King Mongkut's University of Technology North Bangkok, Bangkok, Thailand (e-mail: c.nonchanuttt@gmail.com and prayoot@kmutnb.ac.th).

V. O. Doychinov, I. D. Robertson, and N. Somjit are with the School of Electronic and Electrical Engineering, University of Leeds, Leeds, LS2 9JT, UK (e-mail: v.o.doychinov@leeds.ac.uk, i.d.robertson@leeds.ac.uk and n.somjit@leeds.ac.uk).

There are multiple techniques for thickness characterization of single and multilayer structures, the most popular of which are white-light interferometry and surface profile scanning. Generally, surface profiles in step-height analysis mode are used in cleanrooms to determine the thickness of a deposited dielectric film. However, this method requires contact between the probe stylus and the sample, which could lead to damage of the surface of the film, if the force applied on the stylus is too high. Furthermore, testing multiple samples can be a time-consuming process, as each sample needs to be loaded and unloaded individually and care must be taken not to damage the sensitive probe stylus. This method is also sensitive to mechanical vibrations and special damping measures are required. A white-light interferometer, on the other hand, can offer better resolution than a surface profiler and is often used for high-precision measurements. At the same time, it is also a more expensive instrument that requires even more floor space in a laboratory, as well as specialized personnel training. A white-light interferometer is even more sensitive to mechanical vibrations than a surface profiler and as such is normally housed on solid ground floors. Moreover, the use of white light to measure surface and height profiles necessitates that any photoresist layers have been fully exposed to UV light beforehand; otherwise their properties will change during the course of the measurement.

In this paper, we present an alternative method for non-destructive thickness characterization of dielectric layers deposited on top of glass or quartz substrates. This is achievable through the use of a custom-made hollow rectangular metal waveguide-based sensor integrated with a single complementary split ring resonator (CSRR) fabricated into the top broad wall of the waveguide. This sensor implements the resonance technique, where the change in the resonance frequency of the CSRR, due to dielectric loading provided by the sample under test, is used to determine the thickness of a uniform layer of SU-8 photoresist, deposited onto standard-size laboratory-grade glass substrates. The sensor operates in the WR-10 millimeter-wave frequency band, i.e. 75 – 110 GHz, millimeter-wave measurements are preferred in certain applications, as they can easily penetrate low-loss dielectric materials, such as photoresists, without inducing any chemical reaction and property change as well as achieving high measurement resolution.

For Review Only

The advantages offered by the sensor proposed in this work are several. First of all, working with the sensor does not require complicated training, as the data processing can be automated and staff will only be required to load the sample onto the sensor. The material cost of the sensor, as well as fabrication time, is kept to a minimum by using conventional manufacturing processes. The entire measurement setup takes a fraction of the space required by more expensive instruments, and can be easily relocated as it is not sensitive to mechanical vibrations. Finally, no contact is required with the surface of the sample and there are no restrictions on ambient light conditions. Based on the simulation and measurement results, the thinnest measurable photoresist polymer file is approximately 0.276 µm, which was deemed acceptable for several microfabrication applications such as MEMS devices. The measurement procedure developed for extraction of the photoresist thickness and experimental data show that the sensor in this work can provide an accuracy in excess of 95% when compared to a commercial surface profiler. Although the demonstration of the surface height profiler in this work is based on glass substrates with certain SU-8 photoresist thicknesses, which are limited by materials available in our laboratory, other semiconductor-grade substrates with different polymer thicknesses thicker than 1 µm can be characterized, provided that the dielectric properties of the substrates are well defined. Moreover, higher dielectric-film measurement accuracy can be enhanced by using higher frequencies but this will lead to higher fabrication cost and design complexity due to smaller sensor size.

II. Working Principle, Sensor Design and Fabrication

The sensor structure consists of a custom-made H-plane split WR-10 waveguide block, operating at 75 – 110 GHz. A single CSRR is machined into the top broad wall of the waveguide block. An additional 3D-printed fixture is used for aligning individual samples, which are placed on top of the CSRR. Fig. 1 shows a schematic view of the waveguide sensor in its assembled state, with an outline of a sample under test.

A. Working Principle

The working principle of the sensor is based on one-port S-parameter measurements, reflected and radiated interaction between the standing electromagnetic (EM) wave in the short-circuited waveguide and the multilayered dielectric sample under test, placed on top of the CSRR.

To design the waveguide sensor for operation with the resonance technique, a short-circuited termination is inserted at one of the rectangular waveguide ports. The distance between the CSRR and the short-circuited point is $\lambda_g/4$, where λ_g is the wavelength of the EM signal propagating inside the waveguide at the nominal design frequency of 96 GHz. The design procedure and requirements for the short-circuited termination, implemented as alternating low-impedance and high-impedance sections, are detailed in [7].

By implementing a CSRR into the top-lid of the waveguide with no sample placed on top, i.e. the CSRR is not loaded by

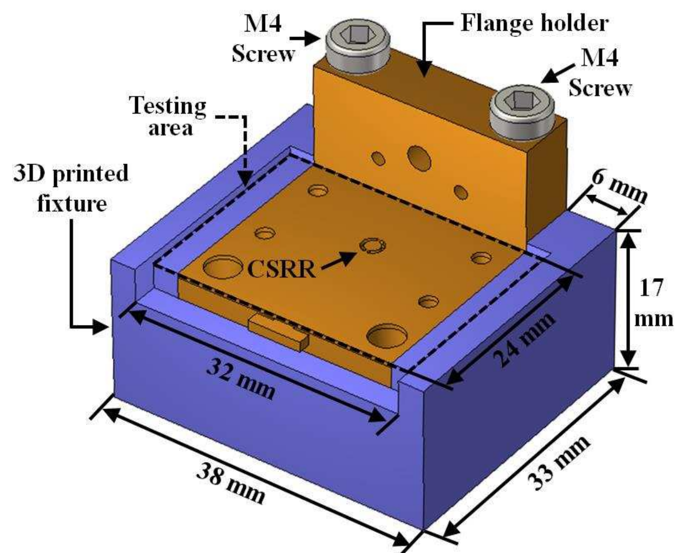

Fig. 1. Schematic view of the tailor-made WR-10 hollow-waveguide thickness characterization and 3D-printed fixture which mounted in bottom part of the sensor to fix the glass substrate during the measurement.

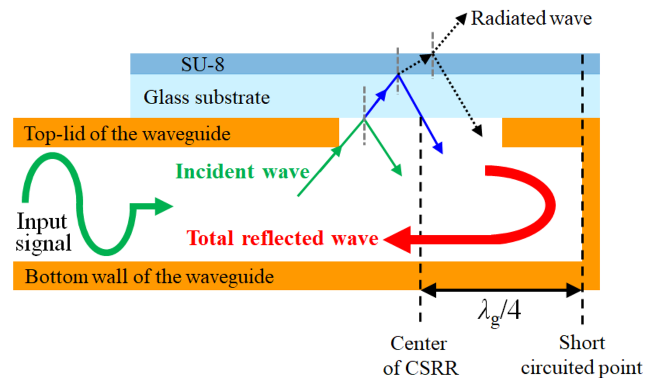

Fig. 2. The EM-wave propagation mechanism after placing a glass substrate coated with SU-8 on top with reflected and radiated EM energy inside the sensor and between free-space, respectively.

the substrate coated by a polymer or dielectric layer, a minimum in the reflected EM energy, $|S_{11}|$, is observed at the operational frequency, 96 GHz, due to the EM-wave radiation into free space. This frequency is referred to as the nominal resonant frequency and is denoted as f_r.

However, when a sample consisting of a multilayered dielectric, such as a substrate with a thin-film dielectric layer deposited on top, is placed on top of the CSRR, a lower resonant frequency shift is observed. The amount by which the resonant frequency shifts is dependent on the thickness of the individual layers and their relative permittivity, and is due to the dielectric loading of the resonator. The EM interaction of the radiated EM wave, show in Fig. 2, when a glass substrate with coated SU-8 is placed on top of the CSRR. Hence, this shift can be used to characterize thin film of dielectric and polymer layers of known materials, such as the widely-used SU-8 photoresist, and determine their thicknesses.

B. Complementary Split Ring Resonator Design

The CSRR is embedded into the top-lid of the waveguide, which is fabricated out of a copper sheet with a thickness of

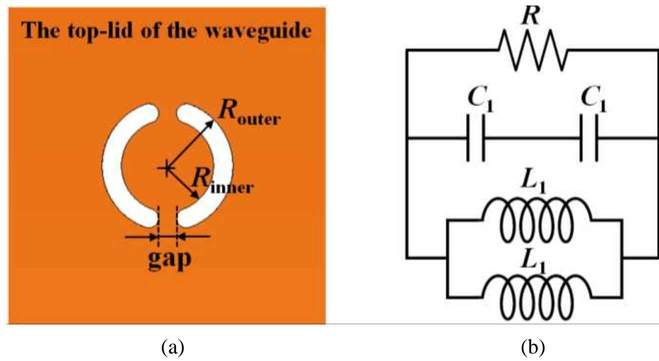

Fig. 3 (a) 2D geometry of the top lid of the waveguide with a CSRR (b) the equivalent circuit model of the CSRR, which is embedded into the top lid of the waveguide.

0.5 mm. The resonator is designed and placed at the middle of the waveguide channel to maximize the electric field around the CSRR slot, resulting in highest electromagnetic radiation of the resonator. Fig. 3 (a) show a 2D geometry of the CSRR, and Fig. 3 (b) depicts the equivalent circuit model of the CSRR structure [18]. The capacitance, contributed by C_1, is due to the slot etched into the top wall, and is dependent on the slot width and overall length. The inductance, denoted by L_1, is contributed by the metal strips denoted as "gap" in Fig. 3 (a). These strips connect the inner metal patches to the rest of the sheet at the top and the bottom of the CSRR. The resistance, represented by R, reflects the losses of the CSRR, and is used to tune the resonant frequency in the reflection coefficient (S_{11}). The values of R_{outer}, R_{inner}, gap, R, C_1, and L_1, optimized by 3D EM simulator (CST Studio Suite) to center the nominal operating frequency at 96 GHz, are 0.64 mm, 0.46 mm, 0.17 mm, 40.1294 Ω, 1.8155 pF, and 6.0156 pH, respectively. In this paper, an operating frequency of 96 GHz is selected as the best compromise between the slot width and gap due to fabrication limitations of the manufacturing facility used.

C. 3D-Printed Fixture

The 3D printed fixture is used to provide a reliable alignment and mechanical stability between the samples under test and the CSRR, ensuring repeatable comparisons between glass substrates coated with SU-8 layers of different thicknesses. During the measurement, the waveguide sensor is fully inserted in the fixture, with the glass substrate being held in place by two recessed pockets. The fixture is 3D printed out of Polylactic acid (PLA) and its geometry, together with the final values of all design parameters of the fixture, are shown in Fig. 1. The mechanical fixture must be designed in the way to avoid any EM interference to the CSRR.

D. Fabrication and Integration

The individual parts of the sensor, shown in Fig. 3, were fabricated in the EPSRC National Facility for Innovative Robotic Systems at the University of Leeds.

The bottom half, which contains the full-sized WR-10 waveguide channel, is machined out of a single copper block using a 5-axis DMU 40 CNC milling machine. The bottom half also has four tapped holes for attaching the upper flange

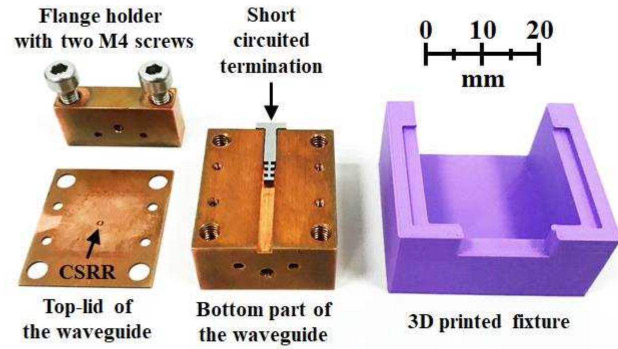

Fig. 4. Fabricated sensor before integration, consisting of the bottom of the waveguide, a single CSRR machined into the top broad wall of the waveguide, flange holder with two M4 screws, the short circuited termination, and 3D printed fixture.

structures and the top lid sheet using fastening screws.

The top lid of the waveguide is fabricated out of a 0.5 mm thick copper sheet, with the CSRR etched into it by using LPKF ProtoLaser U3. Implementing the sensor with this approach provides customization options, by allowing different top lid sheets with different resonator structures to be used and fabricated separately from the bottom waveguide structure. The flange holders, which are mounted on one end of the sensor, were fabricated from a smaller copper block. More information regarding the tailor-made WR10 waveguide fabrication can be found in [8].

The 3D-printed fixture was printed using a CEL Robox RBX02 Dual Material 3D printer out of 1.75 mm diameter PLA filament, using the finest available layer resolution.

To fully assemble the sensor, as presented in Fig. 8, two M4 screws are used to fasten and secure the top half and the flange holders to the bottom half, minimizing air gaps in the H-plane and ensuring good EM performance. At the same time, a standard UG-387/U-M flange [9] is implemented, to ensure correct mating with laboratory measurement equipment. The 3D printed fixture was secured to the waveguide sensor with double-sided adhesive tape. Finally, the assembly is mounted onto a vertical positioner, to be properly connected with the S-parameter measurement equipment.

III. Test Sample Preparation

An attractive material used for microfabrication of passive and microfluidic devices for millimeter-wave and terahertz (THz) frequency applications [10]-[13] is SU-8, which exhibits low loss and the ability to form permanent, high-resolution structures of different thickness. SU-8 is a high-contrast epoxy-based negative photoresist, commonly used in the fabrication of multilayer structures with high aspect ratio (>10:1) [14], and can yield single-layer thicknesses between 0.5 µm and 200 µm. Furthermore, this polymer photoresist exhibits excellent adhesion to inorganic substrates as well as metals that are typically used in microfabrication processes, such as electroplated copper and gold. These features also make SU-8 attractive for future applications such as wafer-level integration of wideband millimeter-wave antennas and digital baseband circuits for system-on-chip (SoC).

Glass substrates with dimensions of approximately 24×32mm^2 and thickness of 160±10 µm were used and coated with SU-8 layers of different thickness in well-controlled cleanroom environment. The samples selected for subsequent S-parameter measurement were chosen based on visual inspection for even and complete SU-8 layer coverage of the glass substrate.

A. Sample Preparation Process

Each individual glass substrate was first cleaned from organic contaminants, which is a standard first step in cleanroom fabrication processes. This helps providing good adhesion between the substrate and the SU-8, and ensures that there are no other substances affecting the S-parameter measurements. The procedure used to clean the glass substrates was as follows:

1. Immerse the sample in a beaker of acetone and rinse in an ultrasonic bath for 5 minutes.
2. Immerse the sample in a beaker of Isopropyl Alcohol (IPA) and rinse in an ultrasonic bath for 5 minutes.
3. Wash the sample in a beaker of DI water for 30 seconds.
4. Dry the sample using a nitrogen blow dry.
5. Perform a de-humidifying bake on a hot plate, set at 120℃, for 5 minutes.

Finally, the thickness of each individual glass substrate was measured independently with an Alpha-Step IQ surface profiler and a calibrated drop-down micrometer.

B. SU-8 Coating

Three different types of SU-8 photoresist were used, in order to obtain a wider range of layer thicknesses. These were SU-8 2002, 2005, and 2010, which are regularly used for microfabrication processes. Prior to processing, the bottles containing the polymer are allowed to reach room temperature and subjected to a 5-minute ultrasonic bath to reduce the air bubbles inside the photoresist. The recipe followed for the subsequent processing for all samples was:

1. Deposit 1 ml of SU-8 onto the glass substrate via pipette.
2. Perform initial spin of 500 rpm for 10 seconds with 100 rpm/s acceleration.
3. Perform the main spin for 30 seconds with 500 rpm/s acceleration. The main spin speed was 3000 rpm for 2002 and 2005; and 3500 rpm for 2010.
4. Perform a soft bake on a hot plate set at 95℃ for 1/2/2.5 minutes for SU-8 2002/2005/2010, respectively.
5. Perform a flood exposure using a Karl Suss MJB3 Mask Aligner with a Mercury lamp, emitting at near UV wavelength of 365 nm, for a total dose of 120/158/188 mJ/cm^2 for SU-8 2002/2005/2010, respectively. The dosage is calculated based on the expected layer thickness and takes into account the transparency of the glass substrate.
6. Perform a post-exposure bake (PEB) on a hot plate set at 95℃ for 2/3/3.5 minutes for SU-8 2002/2005/2010, respectively.
7. Perform a hard bake immediately after the PEB to fully cross-link the polymer, by increasing the temperature of the hot plate to 180℃ with a 5-minute dwell time.

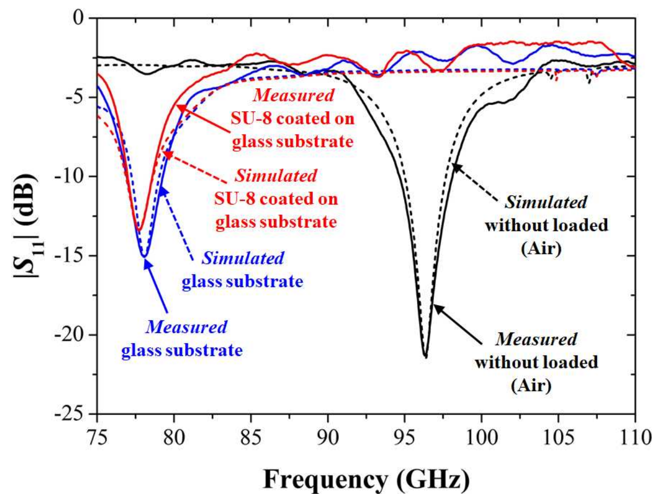

Fig. 5. Simulated (dashed line) and measured (solid line) S_{11} results, for unloaded CSRR (Air), glass substrate, and SU-8 coated on glass substrate.

While the samples investigated in this work were exposed to UV light and baked in accordance with standard operating procedures for SU-8 fabrication, the technique described in Section IV still also works with unexposed and non-baked layers, with the only requirement being that the system is placed in a yellow light room.

Once the sample cooled down to room temperature, the total thickness of the glass substrate plus the SU-8 layer was measured, using the same equipment and methods described in Section III-A.

IV. Thickness Characterization Model

A. Sensor Model Optimization and Material Characterization

In an initial design study conducted by using 3D EM simulation tool CST Studio Suite, the dimensions of the CSRR are designed at the resonant frequency f_r of 96 GHz. After fabrication, the measured result of S_{11} showed that the f_r had shifted to 96.38 GHz, which was attributed to dimension tolerance inaccuracies from the fabrication process. To improve the accuracy of the model based on EM simulations, actual dimensions of the fabricated sensor were measured under high magnification optical microscope and then used to obtain better matching results between measurement and simulation. The final simulated and measured results for $|S_{11}|$ are shown in Fig. 5.

Afterwards, standard lab-grade glass substrates and SU-8 2000 series photoresist are used to develop the thickness characterization model, which requires knowledge of the dielectric properties of the two materials at the frequency band of interest, i.e. 75 – 110 GHz. This process to obtain the value for relative permittivity of glass and SU-8 2000 for the design frequency band consists of the following steps:

For Review Only

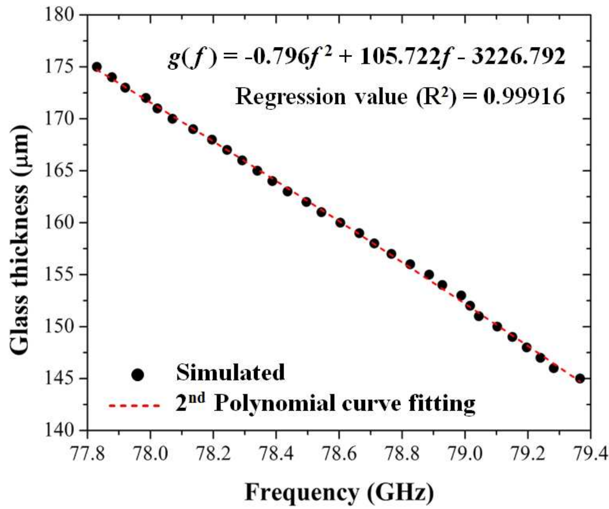

Fig. 6. Glass substrate thickness determination fitted curve as a function of resonant frequency in GHz. The regression value and fitted polynomial, as calculated by Origin, are also annotated.

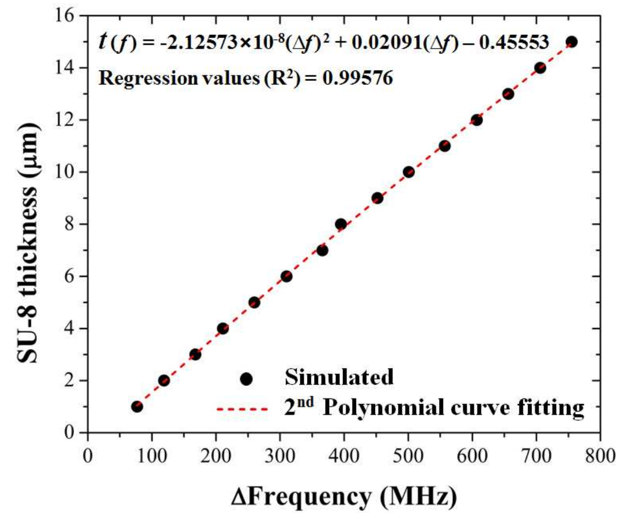

Fig. 7. SU-8 layer thickness determination fitted curve as a function of resonant frequency change in MHz. The regression value and fitted polynomial, as calculated by Origin, are also annotated.

1. Measure the thickness of a glass substrate using an Alpha-Step IQ surface profiler.
2. Measure the S_{11} parameter by loading the CSRR of the sensor with the same glass substrate.
3. Accurately model the physical dimensions of the glass substrate in CST Studio Suite and optimize the value of its relative permittivity until there is a match in the resonant frequency in the $|S_{11}|$, and optimize the value of its loss tangent to match in the magnitude of $|S_{11}|$.
4. Repeat steps 1-3 and change the sample loading the sensor to an SU-8 layer of 13.56 µm deposited on top of the 160.5 µm thick glass substrate.

The simulation results obtained using this process, together with their corresponding S-parameter measurements, are shown in Fig. 5. The relative permittivity and loss tangent of the glass substrate for W-band were investigated to be 4.10 and 0.045, respectively, while the relative permittivity and loss tangent of SU-8 2000 was 3.22 and 0.025, respectively. The results for SU-8 show good agreement with those reported in [15]-[16].

B. Glass Thickness Determination

The numerical technique for extraction of glass substrate thickness from $|S_{11}|$ measurements was also developed using CST Studio Suite.

This was achieved by fixing the values for relative permittivity and loss tangent of glass to 4.10 and 0.045, respectively, and then follow the analysis in Section IV-A. The next step was to sweep the thickness of the glass substrate loading the waveguide sensor from 145 µm to 175 µm in steps of 1 µm. For each simulation, the resonant frequency in $|S_{11}|$ was recorded. A plot of this frequency as a function of glass substrate thickness is presented in Fig. 6.

The next step was to fit these discrete data points to a polynomial by using commercial software package called Origin, where a 2nd order polynomial was found to provide the

TABLE I
EXTRACTION RESULTS OF VARIOUS GLASS SUBSTRATES THICKNESSES

No.	Measured resonance frequency (GHz)	Extracted glass thickness from Eqn. (1) (µm)	Measured glass thickness from Alpha-Step (µm)	% Difference
1	78.955	153.0715	152.75	0.2105
2	78.885	154.4750	154.50	0.0162
3	78.815	155.8708	155.75	0.0776
4	78.670	158.7176	158.20	0.3272
5	78.605	160.0113	160.00	0.0071
6	78.570	160.6946	160.50	0.1212
7	78.570	160.6946	160.50	0.1212
8	78.535	161.3759	161.20	0.1091
9	78.500	162.0552	161.75	0.1887
10	78.255	166.7559	166.50	0.1537

best fit with regression value R^2 of 0.99916. The polynomial itself is given as

$$g(f) = -0.796 f^2 + 105.722 f - 3226.792 \quad (1)$$

where g(f) is the glass substrate thickness in µm as a function of the resonant frequency f_r GHz. A comparison between the fitted and measured values is also shown in Fig. 6. Eqn. (1) can now be used to determine the thickness of glass substrate samples.

C. SU-8 Thickness Characterization

A similar approach was used to develop a relationship between the thickness of the SU-8 layer coated on top of the glass substrates, and the resonance frequency shifts $|\Delta f| = |f_r^{SU-8}| - |f_r^{Glass}|$.

The simulated thickness of the SU-8 photoresist layer was swept from 1 µm to 15 µm with 1-µm steps, while the thickness of the glass substrate was kept constant at 160.5 µm. A 2nd order polynomial was again used, yielding a regression value R^2 of 0.99576. The polynomial itself is

1
2
3
4
5
6
7
8
9
10
11
12
13
14
15
16
17
18
19
20
21
22
23
24
25
26
27
28
29
30
31
32
33
34
35
36
37
38
39
40
41
42
43
44
45
46
47
48
49
50
51
52
53
54
55
56
57
58
59
60

TABLE II
EXTRACTION RESULTS OF VARIOUS SU-8 LAYER THICKNESS

No.	Glass substrate thickness (μm)	Resonant frequency of glass substrate without SU-8 layer (GHz)	Glass substrate plus SU-8 layer thickness (μm)	Resonant frequency of glass substrate with SU-8 layer (GHz)	Relative resonant frequency Δf_r (MHz)	Measured SU-8 layer thickness from Alpha-Step IQ (μm)	Extracted SU-8 layer thickness from Eqn. (2) (μm)	% Difference
1	152.75	78.955	155.25	78.815	140	2.50	2.4715	1.14
2	154.50	78.885	158.25	78.675	210	3.75	3.9346	4.92
3	155.75	78.815	162.08	78.500	315	6.33	6.1290	3.18
4	160.00	78.605	167.75	78.220	385	7.75	7.5917	2.04
5	160.50	78.570	170.70	78.045	525	10.20	10.5164	3.10
6	160.50	78.570	174.06	77.905	665	13.56	13.4402	0.88

$$t(f) = -2.12573\times10^{-8}(\Delta f)^2 + 0.02091\Delta f - 0.45553 \quad (2)$$

where $t(f)$ is the SU-8 thickness in μm as a function of Δf_r, which is in MHz. A plot of the simulated discrete values and fitted polynomial are presented in Fig. 7. Eqn. (1) can now be used together with Eqn. (2) to fully characterize a glass substrate of unknown thickness with a coated SU-8 layer, again of unknown thickness.

V. MEASUREMENT RESULTS

A. Measurement Setup

The S-parameter measurements are obtained by using a Keysight PNA-X N5242A with OML WR-10 VNA Extender Heads. A full two-port calibration was performed using the Thru-Reflect-Line method, in order to eliminate the systematic errors contributed by the PNA-X, connecting cables, and the Extender Heads. The measurements were taken over the entire WR-10 frequency range, i.e. 75 GHz – 110 GHz. Thickness measurements obtained using the Alpha-Step IQ surface profiler [17] were used for comparison and validation proposes. The profiler was configured to run and average three-line scans of 500 μm length, with a transversal scan speed of 10 μm/s and a sampling rate of 100 Hz. Independent of that, a calibrated drop-down micrometer was also used to confirm the Alpha-Step IQ results.

B. Glass Substrates Thickness Measurement

Using the model developed in Eqn. (1), the thickness of the glass substrates is determined from the measured resonant frequency shift. A larger shift in the resonant frequency is observed for a glass substrate with larger thickness. Once the substrate thickness was determined this way, results were compared with the measurements obtained with the Alpha-Step IQ surface profiler, and the difference ratio between the two calculated in percent.

A summary of the measured data and findings is given in Table I. A good agreement is observed between extracted and measured values, which validate the correct and accurate operation of the sensor. The biggest different in glass thickness between two methods was only 0.3272%. The extracted values of the thickness from our measurements were also more consistent than the surface profiler ones in this regard.

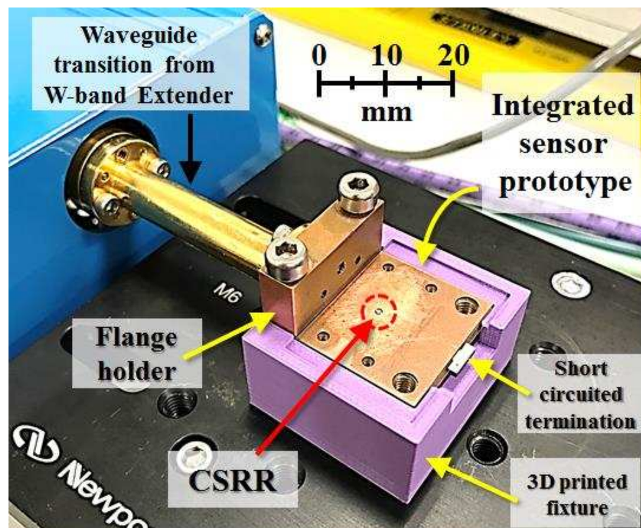

Fig. 8. Fabricated sensor after mounting the 3D printed fixture on the bottom part of the integrated sensor prototype and connecting the sensor to the W-band frequency extender.

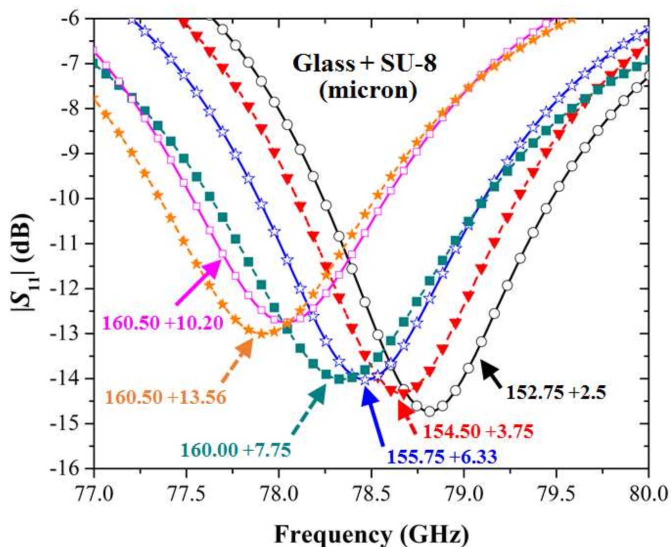

Fig. 9. The measured reflection coefficient S_{11} in dB of the various SU-8 layers coated on glass substrates. The values of the glass substrate thickness plus the SU-8 thickness are annotated for each measurement.

For Review

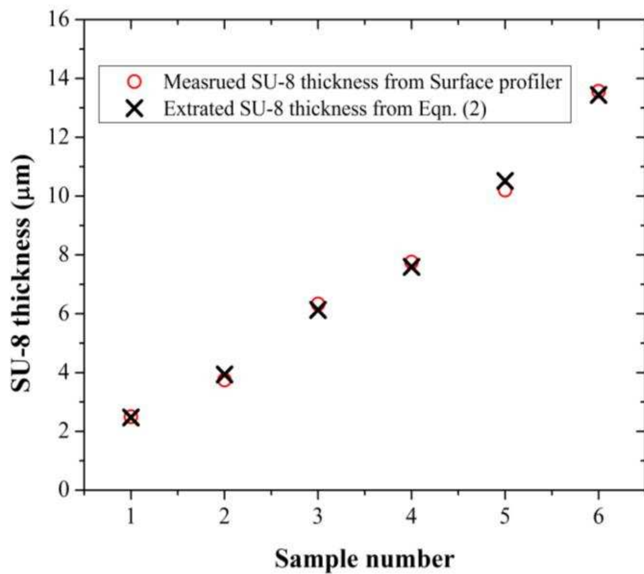

Fig. 10. Comparison between the extracted and measured values of thickness of SU-8 layers coated on glass substrates.

C. SU-8 Layer Thickness Measurement

Six samples of SU-8 layers coated on top of glass substrates were investigated, with thickness as measured by the Alpha-Step IQ of 2.5 µm, 3.75 µm, 6.33 µm, 7.75 µm, 10.20 µm, and 13.56 µm, respectively. The corresponding $|S_{11}|$ measurements of these samples are shown in Fig. 9.

Using the model developed in Eqn. (2), the thickness of SU-8 layers is extracted from the measured data in the following way:

1. Measure the glass substrate without coated SU-8 and record the resonant frequency in the magnitude of S_{11}.
2. Measure the glass substrate with coated SU-8 and calculate Δf_r, which is the difference in resonant frequency between the glass substrate with and without the SU-8 layer.
3. Substitute the value of Δf_r , obtained in the previous step, into Eqn. (2) to calculate the SU-8 layer thickness.

A summary of the experimental results is presented in Table II and Fig. 10. From these it is evident that the proposed sensor achieves a good agreement between extracted and independently confirmed values, which again validate the accurate operation of the sensor. The biggest difference in SU-8 layer thickness between the two methods was only 4.92%. This shows that the sensor retains the accuracy offered by the resonance technique, when adding more dielectric layers on top of the base substrate.

D. Sensor Sensitivity and Limitation

The sensitivity of the SU-8 photoresist thickness characterization sensor can be defined as the ratio between the change in thickness of SU-8 and the change in the resonant frequency, or the slope of the transfer function in Fig. 7. Therefore, the sensitivity of proposed sensor is found to be 0.0214 µm/MHz.

For limitations of the proposed sensor for SU-8 layered thickness measurement, the minimum measurable thickness depends on resolution in measurement setup. In this paper, the measured data are obtained using the Keysight PNA-X N5242A, together with Oleson Microwave W-band frequency extenders by setting 1001 measurement points in 75 – 110 GHz. Using this measurement setup, a frequency change can be detected every 35 MHz, which is the setup choice for fast frequency sweeping. The resolution can calculate by using Eqn. (2). Substituting the value of Δf with 35 MHz, which is the smallest frequency change in the measurement setup for the proposed sensor. Therefore, the smallest SU-8 photoresist film thickness change that can be theoretically detected is 0.276 µm. For the maximum value of the thickness, the proposed can extract photoresist SU-8 layer up to 70 µm, based on the simulation results. At above 70 µm, the S_{11} frequency response will shift lower than 75 GHz, which is lower than the cut-off frequency of the waveguide, causing the measurement frequencies out of the fundamental band (TE_{10} mode) of the WR-10 waveguide. However, the number of measurement points and frequency span (to smaller bandwidth) can be changed to increase the resolution of the sensor; however, this can increase the measurement time. In this paper, 1001 points are used as the best compromise between measurement time and resolution of the sensor due to the performance of equipment available in our laboratory.

VI. Conclusion

A miniaturized custom-made thin-film thickness characterization sensor, operating at the WR-10 millimeter-wave band, has been proposed and its performance investigated and quantified in this work. A single CSRR was found to be sufficient to provide the needed interaction between the standing EM wave and the multilayer samples under test. By loading the CSRR with such a sample, the reflected electromagnetic waves propagating inside the waveguide are changed depending on the relative permittivity of the layer on top of glass substrate and its thickness.

The extracted SU-8 thickness results from the developed numerical model show an excellent agreement when compared with those obtained with a commercial surface profiler, resulting in an accuracy of over 95%. Further advantages of the proposed sensor are reduced measurement time, ease of operation, and contactless mode of operating, as well as potential to measure and characterize unexposed and non-baked photoresist layers. Finally, the frequency range of the sensor can be readily extended to higher waveguide bands, improving its resolution.

Acknowledgment

The authors are grateful to the staff at the EPSRC National Facility for Innovative Robotic Systems for the fabrication of the waveguide and short-circuit structures.

REFERENCES

[1] M. Abou-Khousa and R. Zoughi, "Disbond thickness evaluation employing multiple-frequency near-field microwave measurements," IEEE Trans. Instrum. Meas., vol. 56, no. 4, pp. 1107-1113, Aug. 2007.

[2] M. T. Ghasr, D. Simms, and R. Zoughi, "Multimodal solution for a waveguide radiating into multilayered structures-dielectric property and thickness evaluation," IEEE Trans. Instrum. Meas., vol. 58, no. 5, pp. 1505-1513, May 2009.

[3] Y. Wang, M. Ke, M. J. Lancaster, and F. Huang, "Micromachined millimeter-wave rectangular-coaxial branch-line coupler with enhanced bandwidth," IEEE Trans. Microw. Theory Tech., vol. 57, no. 7, pp. 1655-1660, Jul. 2009.

[4] Y. Li and N. Bowler, "Resonant frequency of a rectangular patch sensor covered with multilayered dielectric structures," IEEE Trans. Antennas Propag., vol. 58, no. 6, pp. 1883-1889, Jun. 2010.

[5] Y. Li, N. Bower, and D. B. Johnson, "A resonant microwave patch sensor for detection of layer thickness or permittivity variations in multilayered dielectric structures," IEEE Sensors J., vol. 11, no. 1, pp. 5-15, Jan. 2011.

[6] C.-S. Lee and C.-L. Yang, "Thickness and Permittivity Measurement in Multi-Layered Dielectric Structures Using Complementary Split-Ring Resonator," IEEE Sensors J., vol. 14, no. 3, pp. 695-700, Mar. 2014.

[7] J. R. Stanec, and N.S. Barker, "A Rectangular-Waveguide Contacting Sliding Short for Terahertz Frequency Applications," IEEE Trans. Microw. Theory Tech., vol. 61, no. 4, pp. 1488-1495, Apr. 2013.

[8] N. Chudpooti, E. Silavwe, P. Akkaraekthalin, I. D. Robertson and N. Somjit, "Nano-Fluidic Millimeter-Wave Lab-on-a-Waveguide Sensor for Liquid-Mixture Characterization," IEEE Sensors J., vol. 18, no. 1, pp. 157-164, Jan. 2018.

[9] Millimeter-Wave Technology & Solutions. Rectangular Waveguide Specification and MIL-Specification Cross Reference [online]. Available: http://www.millitech.com/pdfs/recspec.pdf

[10] H. Sharifi, R. R. Lajiji, H. C. Lin, P. D. Ye, L. P. B. Katehi, and S. Mohammadi, "Characterization of parylene-n as flexible substrate and passivation layer for microwave and millimeter-wave integrated circuits," IEEE Trans. Adv. Packag., vol. 32, no. 1, pp. 84-92, Feb. 2009.

[11] S. Costanzo, I. Venneri, G. Di Massa, and A. Borgia, "Benzocyclobutene as substrate material for planar millimeter-wave structures: Dielectric characterization and application," J. Infrared Milli Terahz Waves, vol. 31, pp. 66-77, 2010.

[12] K. K. Samanta and I. D. Robertson, "Characterization and application of embedded lumped elements in multilayer advanced thick-film multichip-module technology," IET Microw. Antennas Propag., vol. 6, no. 1, pp. 52-59, 2011.

[13] S. Pan and F. Capolino, "Design of a CMOS on-chip slot antenna with extremely flat cavity at 140 GHz," IEEE Antennas Wireless Propag. Lett., vol. 10, pp. 827-830, 2011.

[14] H. Lorenz et al., "High-aspect-ratio, ultrathick, negative-tone near-UV photoresist and its applications for MEMs," Sensor Actuators A, Phys., vol. 64, pp. 33-39, Jan. 1, 1998.

[15] R. G. Pierce, R. Islam, R. M. Henderson, and A. Blanchard, "SU-8 2000 Millimeter Wave Material Characterization," IEEE Microw. Wireless Components Lett., vol. 14, no. 6, pp. 427-429, Jun. 2014.

[16] N. Ghalichechian and K. Sertel, "Permittivity and Loss Characterization of SU-8 Films for mmW and Terahertz Applications," IEEE Antenna Wireless Propag. Lett., vol. 14, pp. 723-726, 2015.

[17] 2010 KLA-Tencor Corporation. Alpha-Step IQ [online]. Available: https://www.kla-tencor.com/ASIQ3_PO_110210_v2.pdf

[18] A. Ebrahimi, W. Withayachumnankul, S. F. A.-Sarawi, and D. Abbott, "Compact Dual-Mode Wideband Filter Based on Complementary Split-Ring Resonator," IEEE Microw. Wireless Components Lett., vol. 24, no.3, pp.152-154, Mar. 2014.

[19] C.-L. Yang, C.-S. Lee, K.-W. Chen, and K.-Z. Chen, "Noncontact Measurement of Complex Permittivity and Thickness by Using Planar Resonators," IEEE Trans. Microw. Theory Tech., vol. 64, no. 1, pp. 247-257, Jan. 2016.

For Review Only